Miscibility and Phase Structure of Blends of Poly(ethylene oxide) with Poly(3-hydroxybutyrate), Poly(3-hydroxypropionate), and Their Copolymers

Yang-Ho Na, Yong He, Naoki Asakawa, Naoko Yoshie, and Yoshio Inoue*

Department of Biomolecular Engineering, Tokyo Institute of Technology, 4259 Nagatsuta, Midori-ku, Yokohama 226-8501, Japan

Received August 28, 2001; Revised Manuscript Received November 5, 2001

ABSTRACT: The miscibility and phase behavior of poly(ethylene oxide) (PEO) blends with poly(3-hydroxybutyrate) (P(3HB)), poly(3-hydroxypropionate) (P(3HP)), and poly(3-hydroxybutyrate-*co*-3-hydroxypropionate)s (P(3HB-*co*-3HP)s) have been investigated by differential scanning calorimetry (DSC) and high-resolution solid-state ^{13}C nuclear magnetic resonance (NMR). Four bacterial P(3HB-*co*-3HP) samples with 3HP contents of 15, 25, 46, and 76 mol % have been used in order to investigate possible influence of the sequence structure of P(3HB-*co*-3HP)s on the miscibility and phase behavior of blends. These four P(3HB-*co*-3HP) samples have different thermal properties and crystallizability depending on the 3HP contents. The DSC thermal behavior of the blends revealed that the blends of PEO with P(3HB), P(3HP), and P(3HB-*co*-3HP)s were miscible over the whole composition range but the crystallization of blend components followed by phase separation exerted much influence on the phase structure of the blends. The results from solid-state NMR spectroscopy showed that the 50/50 binary blends of P(3HB)/PEO, P(3HB-*co*-15%3HP)/PEO, P(3HB-*co*-25%3HP)/PEO, and P(3HP)/PEO were phase-separated due to the presence of crystalline phase but miscible to some extent. Two components in these blend were found to be mixed on a range greater than 30−40 nm, with two crystalline phases and an amorphous phase of miscible two components coexisting.

Introduction

Several kinds of bacteria synthesize and accumulate poly(3-hydroxybutyrate) (P(3HB)) as a reserve material which can be harmlessly biodegraded to water and carbon dioxide by a wide variety of microorganisms in the environment.[1−4] Bacterial P(3HB) has attracted much industrial attention as an environmentally degradable thermoplastic for a wide range of agricultural, marine, and medical applications but suffers two limitations in its use: a very narrow processability window and a relatively low impact resistance.[5−7] Blending of P(3HB) with suitable polymers may improve its impact resistance and decrease the melting point, which implies the possibility of processing the materials at a lower temperature to avoid thermal degradation of P(3HB). Poly(ethylene oxide) (PEO)/P(3HB) is an example of attempts to improve the physical and thermal properties of P(3HB) by blending with synthetic or natural polymers. The compatibility, the phase structure, the rheological properties, and the enzymatic degradation of P(3HB)/PEO blend have been investigated.[8−13] In previous reports, it has been reported that P(3HB) and PEO are miscible in the melt state and in the amorphous state.

Recently, He et al. investigated the phase behavior of high molecular weight PEO (M_v = 300 000) with chemosynthesized poly(3-hydroxypropionate) (P(3HP)) and bacterial P(3HB) by differential scanning calorimetry (DSC), dynamic mechanical thermal analysis (DMTA), and high-resolution solid-state ^{13}C nuclear magnetic resonance (NMR).[14] They found that high molecular weight PEO is miscible with P(3HP) over the whole composition range while it is partly miscible or immiscible with bacterial P(3HB). Because of the difference between miscibility of P(3HB)/PEO and P(3HP)/PEO blend systems, it is of great interest to investigate the effect of sequence structure of bacterial poly(3-hydroxybutyrate-*co*-3-hydroxypropionate) (P(3HB-*co*-3HP)) copolymers on the miscibility of P(3HB-*co*-3HP)/PEO blend systems. Chemical structures of P(3HB-*co*-3HP) and PEO are shown in Figure 1. It is thought that the miscibility of PEO blends with P(3HB-*co*-3HP) may be dependent on the 3HP contents of copolymers and the morphology of these blends will be influenced by their phase structure. In other words, by a choice of P(3HB-*co*-3HP)s with proper 3HP content, the physical and thermal properties and biodegradation rate, resulting from structural changes of blend systems, can be regulated. On the other hand, it is also necessary to indicate that though He and his colleagues' experiments have been conducted under the presence of high extents of crystalline phases of blends, there have been few discussions about the probability of phase-separation by crystallization of each blend component and its effect on miscibility of P(3HB)/PEO or P(3HP)/PEO blends. It is worthwhile to discuss this phase-separation phenomena in that P(3HB) and P(3HP), as well as PEO, are all highly crystalline polymers.

Recently, it has been known that comonomer composition as well as comonomer compositional distribution are also important factors regulating the morphology and physical properties of P(3HB-*co*-3HP) copolymers. Cao et al., based on the wide-angle X-ray diffraction of P(3HB-*co*-3HP)s, have reported that 3HB-rich (0-38.3 mol % 3HP) and 3HP-rich (77.9−100 mol % 3HP) copolyesters form distinct helix structures, while copolyesters with 3HP content ranging from about 45−75 mol % appear as the amorphous state.[15] According to our recent study of binary blends between composi-

* To whom correspondence should be addressed.

10.1021/ma011530y CCC: $22.00
Published on Web 01/03/2002

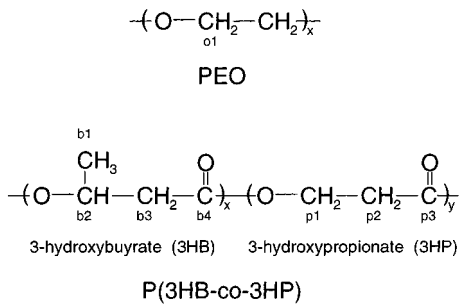

Figure 1. Chemical structures of PEO and P(3HB-*co*-3HP).

tionally fractionated P(3HB-*co*-3HP) samples,[16] it was found that the miscibility mainly depends on the difference of 3HP contents between the two components of the blend. It was also found that the type of crystalline lattice, miscibility, and difference of the spherulite growth rate are the important factors controlling the crystalline phase behavior. Hence, to elucidate correlation between the structure and the physical properties of P(3HB-*co*-3HP) blends, an investigation of phase behavior with the change of comonomer composition are needed for strict physical characterization of the P(3HB-*co*-3HP) blends.

In this paper, we shall study the blend compositional dependence of the miscibility and the morphology of the P(3HB)/PEO, P(3HB-*co*-3HP)/PEO, and P(3HP)/PEO binary blends by the methods of DSC thermal analysis and high-resolution solid-state NMR spectroscopy. The effect of crystalline phases of components in the binary blends on the phase behavior and miscibility level will be also discussed.

Experimental Section

Materials. The PEO and bacterial-origin P(3HB) samples were purchased from Aldrich Chemical Co. The P(3HB) sample was used after purification in ethanol from 1,2-dichloroethane solution. The PEO sample was used as received. The P(3HP) sample, chemically synthesized through a ring opening polymerization of propiolactone, was supplied by Tokuyama Co. (Tsukuba, Japan), which was also purified with chloroform and *n*-hexane. Three kinds of P(3HB-*co*-3HP) samples with 3HP contents of 19, 20, and 61 mol % were originally biosynthesized by the bacteria *Alcaligenus latus* (ATCC 29713) from the mixed carbon substrates of (*R*)-3-hydroxybutyric acid ((*R*)-3HBA) and 3-hydroxypropionic acid (3HPA) through an one-stage fermentation. The pH value of the cultivation medium was regulated to be 7.0 with 2 M NaOH and 2 M H_2SO_4. After bacterial cells were harvested by centrifugation, copolyesters were extracted from the lyophilized cells with hot chloroform using a Soxhlet apparatus and purified by reprecipitation with ethanol. Comonomer compositional fractionation of as-produced P(3HB-*co*-3HP) sample was carried out in chloroform(solvent)/*n*-heptane(nonsolvent) mixed solvents. A small amount of *n*-heptane was carefully added stepwise to the chloroform solution under gentle agitation at 0−2 °C. The precipitated mass was isolated by centrifugation (8000 rpm, 30 min). This procedure was repeated until the addition of a large amount of *n*-heptane hardly caused any appreciable precipitation. The procedures of biosynthesis and fractionation have been described in details in our previous works.[15,17,18] Four compositionally fractionated copolyesters, for which the 3HP content was 15, 25, 46, and 76 mol % respectively, were selected for the investigation of blend samples between PEO and P(3HB-*co*-3HP). The molecular characteristics of P(3HB), P(3HP), four fractionated P(3HB-*co*-3HP)s, and PEO are tabulated in Table 1. Hereafter, P(3HB-*co*-3HP) with 3HP content of 15 mol %, for example, will be shown as P(3HB-*co*-15%3HP).

Preparation of Blend Samples. P(3HB), P(3HP), PEO, four selected P(3HB-*co*-3HP)s, and the binary blends between

Table 1. Characteristics of Polymer Samples

sample	3HP content (mol %)[d]	M_n ($\times 10^{-5}$)[e]	M_w/M_n[e]
P(3HB)[a]	0	1.44	2.78
P(3HB-*co*-15%3HP)[a,b]	15	1.67	2.29
P(3HB-*co*-25%3HP)[a,b]	25	0.95	2.19
P(3HB-*co*-46%3HP)[a,b]	46	1.05	6.52
P(3HB-*co*-76%3HP)[a,b]	76	2.33	2.80
P(3HP)[c]	100	0.93	2.25
PEO[c]		3.0 (M_v)	2.47

[a] Bacterial origin. [b] Fractionated. [c] Chemosynthetic. [d] Determined by ^{1}H NMR. [e] Determined by GPC.

(co)poly(hydroxyalkanoate)s and PEO with weight ratios of 90/10, 75/25, 50/50, 25/75, and 10/90 were first dissolved in chloroform (2 wt %) and the solutions were cast on the Teflon dishes as casting surfaces. After casting, the solvent was allowed to evaporate at room-temperature overnight, and then the blends were dried in the oven at 45 °C under vacuum for 2 days to remove the residual solvents. All obtained films were aged at room temperature for 1 month before physical characterization was attempted.

Analytical Procedures. Molecular weights of polyester samples were measured by a Tosoh HLC-8020 GPC instrument with a Tosoh SC-8010 controller, refractive detector and TSK gel $G2000H_{XL}$ and GMH_{XL} columns. Polystyrene standards with narrow molecular-weight distribution were used to construct a calibration curve, then the number average and weight average molecular weight (M_n, M_w) and polydispersity (M_w/M_n) were calculated.

The 3HP molar fractions of the P(3HB-*co*-3HP) samples were determined from the ^{1}H NMR spectra measured on a Varian Unity 400 NMR spectrometer at 400 MHz and 25 °C in $CDCl_3$ solution with a 4.8 μs pulse width (45° pulse), 5 s pulse repetition time, 6000 Hz spectral width, 64K data points, and 32 FID accumulations.

Thermal analyses were conducted on a Seiko DSC200U controlled by a Seiko EXSTAR6000 workstation. The melting temperature (T_m) and enthalpy of fusion (ΔH) were estimated from the DSC thermal traces measured by heating the samples from −100 to +195 °C at a rate of 20 °C min^{-1} (first scan). After rapid quenching, the glass transition temperature (T_g) was measured by reheating the samples from −100 to +195 °C at a rate of 20 °C min^{-1} (second scan). The melting peak temperature was determined from the endothermic peak of the DSC curve recorded in the first scan, and the value of the heat of fusion was calculated as the integral of the endothermic peak in the DSC curve. The T_g value was estimated as the midpoint of heat capacity change in the thermal diagram obtained by the second heating scan.

High-resolution solid-state ^{13}C NMR spectra were measured at room temperature on a Varian Unity 400 NMR spectrometer at 100.6 MHz for ^{13}C nucleus. Proton spin−lattice relaxation times in the laboratory frame (T_1^H) was determined by an inversion−recovery pulse sequence ($\pi-\tau-\pi/2$) followed by cross-polarization (CP) to ^{13}C magnetization. The spectra were measured under high-power proton dipolar decoupling(ca. 59.5 kHz). The pulse recycle delay was 5 s after a 90° flip back pulse. The magic angle spinning(MAS) rate was 5.0 kHz (±0.1 kHz) and ^{1}H−^{13}C contact time was 5 ms. A total of 512−1024 free induction decays (FID) were accumulated. ^{13}C NMR chemical shifts were reported in ppm relative to tetramethylsilane (TMS) by taking the methyl carbon of hexamethylbezene (17.4 ppm) as an external reference.

Results and Discussion

Thermal Behavior. The glass transition temperature (T_g), cold crystallization peak temperature (T_{cc}), melting temperature (T_m), and enthalpy of fusion (ΔH) of binary blends of PEO with P(3HB) and its copolymer were determined from DSC thermograms. The results are summarized in Table 2. As typical examples, Figures

Table 2. Thermal Properties of PEO Blends with P(3HB), P(3HP), and P(3HB-*co*-3HP)s

sample	composition P(3HB-*co*-3HP)/PEO	T_g/°C P(3HB-*co*-3HP)	T_{cc}/°C PEO	T_m/°C P(3HB-*co*-3HP)	T_m/°C PEO	ΔH/(J g^{-1}) P(3HB-*co*-3HP)	ΔH/(J g^{-1}) PEO
P(3HP)/PEO	100/0	−20	15	69, 78, 84	···	74	
	90/10	−22	14	78, 86	67	79	
	75/25	−25	18	77, 86	68	90	
	50/50	−28	16	76, 85	68	115	
	25/75	−32			69	130	
	10/90	−41			71	134	
	0/100	−49			70		150
P(3HB-*co*-76%3HP)/PEO	100/0	−11		43		6	
	90/10	−16		42	59	23	
	75/25	−23	12	42	61	44	
	50/50	−25			63	64	
	25/75	−29			71	110	
	10/90	−36			71	142	
	0/100	−49			70		150
P(3HB-*co*-46%3HP)/PEO	100/0	−2		59		17	
	90/10	−11			60	21	
	75/25	−13			64	49	
	50/50	−16			71	92	
	25/75	−25			68	127	
	10/90	−37			69	141	
	0/100	−49			70		150
P(3HB-*co*-25%3HP)/PEO	100/0	0		100		48	
	90/10	−7		102	67	20	10
	75/25	−15		101	67	9	30
	50/50	−14		100	69	5	71
	25/75	−24		97	70	2	113
	10/90	−37		n.d.	72	n.d.	140
	0/100	−49			70		150
P(3HB-*co*-15%3HP)/PEO	100/0	4	72	132, 145		59	
	90/10	−4	53	134, 146	60	28	18
	75/25	−10	17, 46	136, 146	69	25	33
	50/50	−11	46	134, 145	69	16	73
	25/75	−25		129, 143	69	9	120
	10/90	−36		n.d.	71	n.d.	137
	0/100	−49			70		150
P(3HB)/PEO	100/0	7	60	163, 176		86	
	90/10	−6	38	162, 176	65	35	8
	75/25	−17	4, 34	163, 176	65	34	24
	50/50	−23	33	163, 176	69	26	81
	25/75	−42		164, 174	69	5	119
	10/90	−43		174	69	n.d.	135
	0/100	−49			70		150

2 and 3 show the DSC traces of homopolymer P(3HB), PEO, and blends with various constituent compositions recorded by the first and second heating scan, respectively.

The T_g value of P(3HB) was 7 °C, and those of P(3HB-*co*-3HP) copolymers and P(3HP) samples decreased up to −20 °C as the 3HP molar fraction increased. As can be seen from Table 2, all the blends showed a single T_g, and the T_g value decreased from +7 to −49 °C with an increase in the amount of the PEO component. Blend miscibility is often quantified by measuring the blend T_g and by analyzing its compositional dependence. Traditionally, the equations based on the free volume hypothesis have been used to model the compositional dependence of the glass transition temperature. One of mostly used expressions is the Gorden−Taylor equations,[19] rederived by Wood,[20] as follows

$$T_g = \frac{W_1 T_{g1} + k W_2 T_{g2}}{W_1 + k W_2} \quad (1)$$

where W_1, W_2 are the weight fractions and, T_{g1}, T_{g2} are the glass transition temperatures of the component polymers 1 and 2 of the blend and T_g is the glass transition temperature of the blend with a fitting parameter k. $k = \Delta C_{p2}/\Delta C_{p1}$, and ΔC_{pi} is the glass transition increment of the heat capacity of the speci-

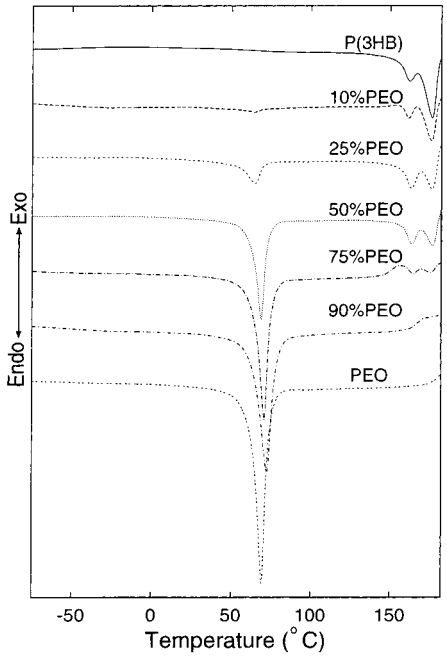

Figure 2. DSC thermograms of the pure polymers P(3HB), PEO, and binary P(3HB)/PEO blends measured by the first heating scan.

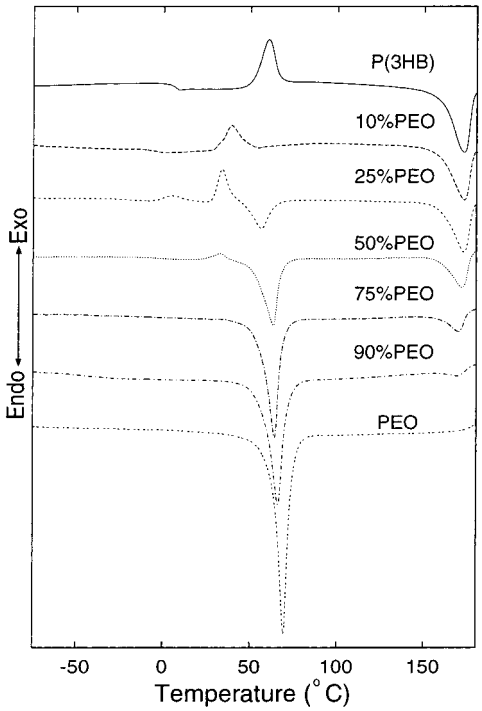

Figure 3. DSC thermograms of the pure polymers P(3HB), PEO, and binary P(3HB)/PEO blends measured by the second heating scan.

men, originally assumed to be independent of temperature. This classical equation predicts that T_g changes continuously and monotonically with composition.

Solid lines (line 1) of Figure 4, parts a−f, show compositional dependence of T_g for PEO blends with P(3HB), P(3HP), and P(3HB-*co*-3HP) copolymers. As far as the T_g of Figure 4 is concerned, it emerged from DSC analysis that the blends are characterized by a single T_g intermediate between those of two components. The T_g values, which are in general agreement with those calculated from the above equation, are composition dependent. Equation 1, as shown in Figure 4, fits the experimental T_g data well. Considering the previous studies of P(3HB)/PEO or P(3HP)/PEO blends,[8−14] in which were reported that these blend systems are miscible or at least partially miscible, it is satisfactory to consider that the PEO blend systems with P(3HB) and P(3HB-*co*-3HP) copolymers are miscible in the melt and in the amorphous state.

For solid lines (line 1) of Figure 4, parts a−e, it seemed abnormal that the blends of PEO content 10% and 25% possessed lower T_gs than those expected by the Wood equation. Figure 5 is given to help the explanation about this. The P(3HB-*co*-76% 3HP)/PEO 90/10 blend showed a small melting peak for the PEO component as well as the bacterial copolymer component. In the DSC curve of P(3HB-*co*-76% 3HP) 75/25 blend, a crystallization peak appeared after the glass transition, and the area of this peak was almost the same as that of the melting peak. These results indicated that both the 90/10 and 75/25 blends were in the fully amorphous state before the occurrence of glass transition during the second heating scan. In contrast, there were no crystallization peak of the PEO component after the glass transition in the DSC curve of the other blends; that is, the crystallization was completed during quenching just as for pure PEO. It is well-known that the crystallization of a polymer causes an increase in its T_g as the crystallization lowers the mobility of the polymer chains in the amorphous phase.[21] So, it should be acceptable to attribute the anomaly mentioned above to the difference in the phase structure; that is, P(3HB-*co*-76% 3HP) 90/10 and 75/25 blends were in the amorphous state before the glass transition whereas the other blends were in the semicrystalline state.

Table 3 lists the k, k', and k'' values of empirical adjustable parameter which is calculated from the Wood equation. k was calculated over the whole compositionn and the k' value was that calculated by only using T_gs of two homo(co)polymers and, 90/10 and 75/25 blends thought to be in the amorphous state. The k'' value was obtained from all data excluding the two amorphous ones. Figure 4 shows the difference of T_g−composition curves with various fitting parameters—k, k', and k''. As mentioned above, it suggested that the T_gs depend on phase structural properties, particularly crystallinity.

The k and k'' values of P(3HB-*co*-15%3HP)/PEO, P(3HB-*co*-25%3HP)/PEO, P(3HB-*co*-46%3HP)/PEO, and P(3HB-*co*-76%3HP)/PEO blend system are almost the same each other, that is, 2.2−2.5 and 0.7−0.9, respectively. Moreover, the k' values have slight differences of 0.4−1.6 even for all blend systems. Thus it can be considered that there is little effect of the change of 3HP contents on the k, k', and k'' values. If it is assumed that T_g−composition data are expressed with equations which predict a monotonic variation of T_g and any deviation of the results from the linear behavior is then considered as a measure of the strength of the interactions involved, the addition of 3HP monomer units makes little effects on the miscibility of P(3HB-*co*-3HP) copolymer blends with PEO. This result seems to be reasonable because the specific interactions responsible for P(3HB)/PEO miscibility may involve the carbonyl groups of P(3HB) and the hydrogen of the CH_2 group of PEO, suggested by Avella and co-workers,[8] and P(3HP) has a chemical structure to that of P(3HB). To examine the miscibility of P(3HB-*co*-3HP) copolymer blends with PEO more clearly, such experiments as solubility parameter measurements and spectroscopic methods are needed.

As listed in Table 2, the T_m values of PEO and P(3HB-*co*-3HP) copolymers decreased after blending, as a general trend. For the PEO components, the T_m showed a decrease of from 3 (P(3HP)/PEO) to 11 °C (P(3HB-*co*-76%3HP)) for each blend system with each change in content. In contrast, the T_m values of P(3HB), P(3HP), and its copolymer component showed smaller decrease than PEO component with the increase of the content of PEO. It is worth pointing out that the T_m observed here are not equilibrium points nor those of samples crystallized isothermally. Here it is meaningful to describe other examples. Isotactic polystyrene (i-PS) and poly(methyl metacrylate) (PMMA) are not miscible but the i-PS single crystals show a T_m depression when embedded in PMMA.[22] Conversely, miscible blends of PEO and PMMA do not show a clear decrease of T_m for PEO. Therefore it should also be indicated that the T_m decrease alone is not absolute proof of miscibility.[23] To show the dependence of equilibrium T_m and the crystallizability on composition more clearly, some observations were performed in different heat-treatment conditions.

Table 4 lists the melting temperatures, the heats of fusion and the calculated crystallinities of P(3HB)/PEO blends prepared by conventional solvent-casting method

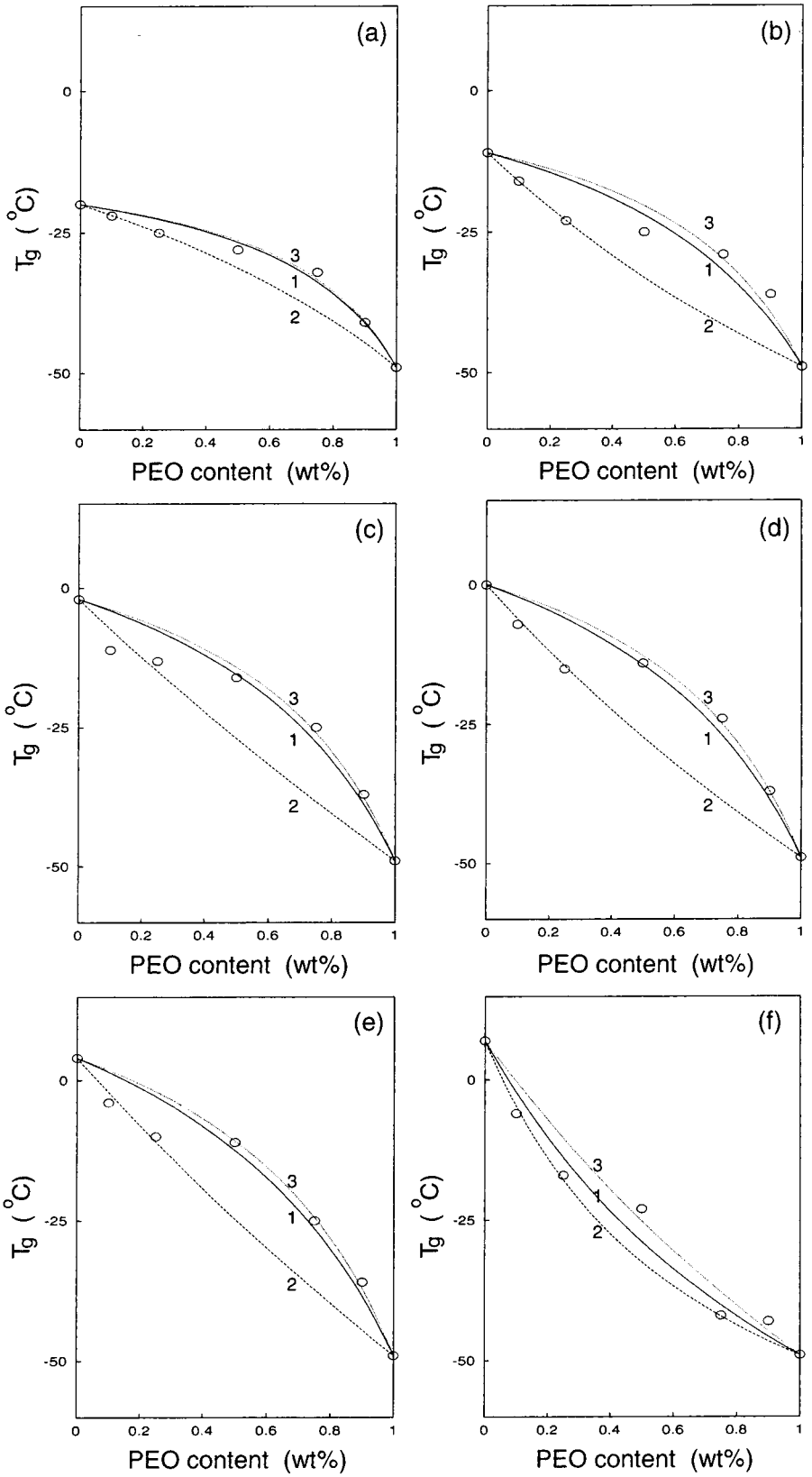

Figure 4. Compositional dependence of glass transition temperature for blends of (a) P(3HP)/PEO, (b) P(3HB-*co*-76%3HP)/PEO, (c) P(3HB-*co*-46%3HP)/PEO, (d) P(3HB-*co*-25%3HP)/PEO, (e) P(3HB-*co*-15%3HP)/PEO, and (f) P(3HB)/PEO. The solid line (line 1) indicates the results over the whole composition calculated by the Wood equation. The dashed line (line 2) shows the ones that were calculated by only using T_gs of two homo(co)polymers and 90/10 and 75/25 blends. The dotted line (line 3) shows the ones obtained from all data excluding the two amorphous ones.

as mentioned in Experimental Section and aged in 80 °C for 1 month after casting and drying, respectively. (the degree of crystallinity was calculated by taking 205 and 146.6 J g^{-1} as the melting enthalpies for 100% crystalline PEO[24] and P(3HB)[25] components, respectively.) It was obvious that the T_m values of both P(3HB)

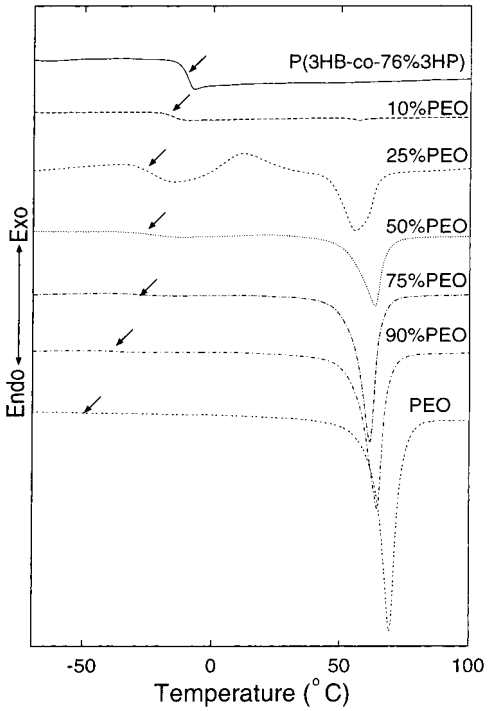

Figure 5. DSC thermograms of the pure polymers P(3HB-*co*-76%3HP), PEO, and binary P(3HB-*co*-76%3HP)/PEO blends measured by the second heating scan. The arrow indicates the glass transition temperature of P(3HB-*co*-76%3HP) and P(3HB-*co*-76%3HP)/PEO blends and PEO.

Table 3. Values of Fitting Parameters, *k*, *k′*, and *k″* of PEO Blends with P(3HB), P(3HP), and P(3HB-*co*-3HP)s

sample	*k*	*k′*	*k″*
P(3HP)/PEO	3.3(±0.4)	1.6(±0.0)	3.5(±0.4)
P(3HB-*co*-76%3HP)/PEO	2.5(±0.7)	0.7(±0.0)	3.0(±0.6)
P(3HB-*co*-46%3HP)/PEO	2.5(±0.5)	0.9(±0.2)	2.9(±0.2)
P(3HB-*co*-25%3HP)/PEO	2.4(±0.5)	0.8(±0.0)	2.9(±0.1)
P(3HB-*co*-15%3HP)/PEO	2.2(±0.4)	0.8(±0.1)	2.6(±0.1)
P(3HB)/PEO	0.6(±0.1)	0.4(±0.0)	0.7(±0.1)

and PEO components in the P(3HB)/PEO blends aged at 80 °C were larger, a decrease of about 12 °C from those for P(3HB)/PEO blends prepared at room temperature. These results showed that the crystallization of P(3HB) was greatly affected by PEO. Since PEO is in the amorphous state at 80 °C, above the T_m value of PEO, this decrease of the T_m value may be an indirect proof of miscibility between P(3HB) and PEO, indicating the presence of some intermolecular interactions. It may be seen that the crystallinities of each component in the P(3HB)/PEO blend aged at room temperature and in that aged at 80 °C decrease with the decrease of each content in the blend. The decrease of crystallinity may be mainly attributed to the mutual dilution effect and the influence of melt compatibility on the crystallization process.

Thermal properties of crystalline part in the blends of PEO with P(3HB), P(3HP), and P(3HB-*co*-3HP) copolymers depend on the microstructure of the blends which is influenced by the mobility and the crystal growth rate of respective components.[16,26,27] PEO has a significantly lower T_g (and higher molecular weight) and higher crystallization rate if compared with P(3HB) and P(3HB-*co*-3HP)s to be measured by spherulite growth rate.[16,27] In addition, P(3HB-*co*-3HP) (co)polymers exhibit complex physical properties with the change of 3HP contents; with the increase of 3HP contents, the T_g of P(3HB-*co*-3HP)s decreases, and the crystallization rate of P(3HB-*co*-3HP)s decreases at first for 3HB-rich (ca. 0−40 mol %) copolyesters and then increases for 3HP-rich (ca. 75−100 mol %) copolyesters.[15] Hence, crystalline structure of P(3HB-*co*-3HP)/PEO blends depends on the relationship between the mobility of amorphous components and difference of crystallization rate. In crystallization process, low-T_g PEO may diffuse away outside and reside in intraspherulite region (the results of optical observation were not shown.), and then grow faster than P(3HB-*co*-3HP)s.[9,10] For P(3HB-*co*-45%3HP)/PEO and P(3HB-*co*-76%3HP)/PEO blends, it is expected that only PEO lamella may grow in the initial stage but P(3HB-*co*-45%3HP) and P(3HB-*co*-76%3HP) may be trapped in the PEO spherulites due to higher T_g and appreciably lower crystal growth rates of P(3HB-*co*-3HP)s.

Proton Spin—Lattice Relaxation Behavior. High-resolution solid-state ^{13}C NMR measurements were carried out to characterize the solid structure of PEO blends with P(3HB), P(3HB-*co*-15%3HP), P(3HB-*co*-25%3HP), and P(3HP). The samples as mentioned in Experimental Section were used in the solid-state NMR experiments. Figures 6 and 7 show the conventional CP/MAS ^{13}C NMR spectra of the investigated samples. For P(3HB)/PEO 50/50 blend (Figure 6), P(3HB) signals are broadened. It may be caused by the following two reasons, that is, the diversification of conformation of the P(3HB) chain and the reduction of the rf decoupling of C−H dipolar interactions, both resulting from an increase of the amorphous portion.[28,29]

Measurement of the proton spin−lattice relaxation time for the specific carbons in the blend permits analysis and identification of microheterogeneous structures in terms of the difference in their relaxation behavior.[30−32] In addition, the relaxation of the heterophase domains can be evaluated based on the spin diffusion phenomenon. In this article, the values of proton spin−lattice relaxation times in the laboratory frame (T_1^H) were used to discuss the miscibility of blends. Figure 8 depicts the stacked ^{13}C NMR spectra of the P(3HB-*co*-15%3HP)/PEO 50/50 blend as a function of time delay τ after a π-pulse in the inversion−recovery sequence. In principle, the apparent ^{13}C magnetization at each specific site is indirectly associated with proton magnetization locked in the ^1H channel through cross-polarization under the matched Hartmann−Hahn condition, and the decays in a manner mathematically described as[33]

$$M(\tau) = M_\infty[1 - 2\exp(-\tau/T_1^H)] \qquad (2)$$

in which $M(\tau)$ and $M(\infty)$ represent intensities of the carbon resonance at a given time delay τ and equilibrium state ($\tau > 5T_1^H$), respectively; T_1^H expresses the proton spin−lattice relaxation in the laboratory frame. Further, eq 3 can be rearranged as

$$\ln[M_\infty - M(\tau)] = -\tau/T_1^H + \ln(2M_\infty) \qquad (3)$$

By plotting of $\ln[M_\infty - M(\tau)/(2M_\infty)]$ against time delay τ, straight lines with different slopes were obtained corresponding to the (co)polymers, indicating a single component T_1^H relaxation behavior. The T_1^H values for the component of blends were calculated from the slopes of the straight lines.

Table 4. Melting Temperature, Melting Enthalpy, and Crystallinity of PEO/P(3HB) Blends Aged at Room Temperature and 80 °C

sample	composition P(3HB)/PEO	T_m/°C		ΔH/(J g^{-1})		X_c/%	
		P(3HB)	PEO	P(3HB)	PEO	P(3HB)	PEO
P(3HB)/PEO	100/0	163, 176		86		59	
aged at room	90/10	162, 176	65	35	8	27	39
temperature	75/25	163, 176	65	34	24	31	48
	50/50	163, 176	69	26	81	35	79
	25/75	164, 174	69	5	119	12	78
	10/90	174	69	n.d	135	n.d.	73
	0/100		70		150		73
P(3HB)/PEO	100/0	167, 178		81		55	
aged at 80 °C	90/10	163, 175	54	78	3	59	15
	75/25	159, 170	55	53	8	49	16
	50/50	156, 164	64	15	32	20	31
	25/75	161, 171	57	8	84	21	54
	10/90	165	53	4	81	27	44
	0/100		66		140		68

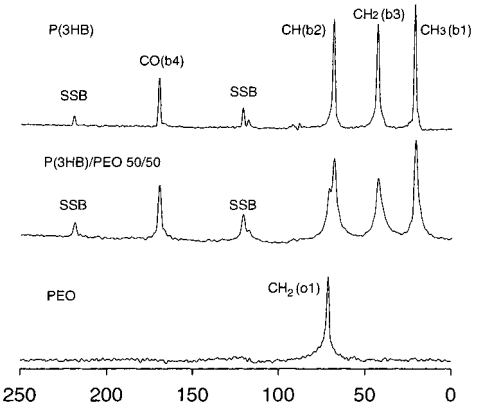

Figure 6. ^{13}C CP/MAS NMR spectra for P(3HB), P(3HB)/PEO 50/50 blend, and PEO. The peaks marked by SSB indicate the spinning sidebands.

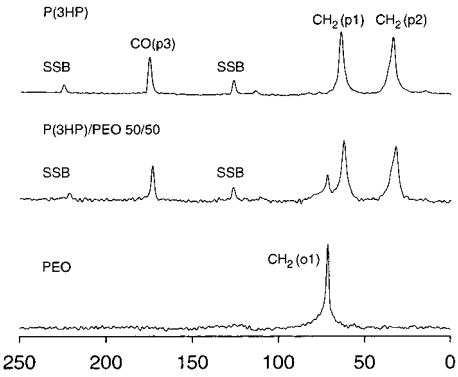

Figure 7. ^{13}C CP/MAS NMR spectra for P(3HP), P(3HP)/PEO 50/50 blend and PEO. The peaks marked by SSB indicate the spinning sidebands.

Tables 5 and 6 shows the T_1^H values of homo(co)-polymers and those of 50/50 blend samples of P(3HB)/PEO, P(3HB-*co*-15%3HP)/PEO, P(3HB-*co*-25%3HP)/PEO, and P(3HP)/PEO blend systems. The T_1^Hs values of the CH_3(b1) site of P(3HB), P(3HB-*co*-15%3HP), and P(3HB-*co*-25%3HP) are 1.76, 1.64, and 1.19 s, respectively. Other carbon sites have a similar tendency to those of CH_3 site. For 3HB-rich copolyesters, as the composition of the 3HP monomer increased, the value of T_1^H decreased. Cao et al. have reported that P(3HB-*co*-3HP)s have the same P(3HB) type of crystal lattice structure, and those crystallinities decrease with increase of 3HP mole fraction in the range of 3HP mole fraction from 0 to 38.3%.[15] The decrease of the T_1^H value for P(3HB) and P(3HB-*co*-3HP) copolymers may reflect the increase in the extent of proton spin-diffusion and the increase of amorphous parts by adding 3HP monomer units may be one reason of the change of proton spin-diffusion. On the other hand, the T_1^H value of P(3HP) is larger than those of P(3HB). It can be thought that it results from the difference of chemical structure, that is, more chain-flexibility by the absence of the side CH_3 group.

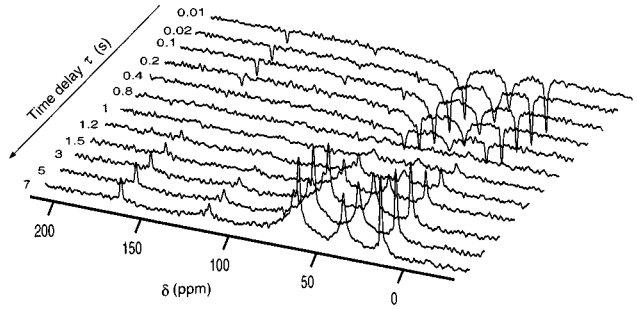

Figure 8. ^{13}C NMR spectra for P(3HB-*co*-15%3HP)/PEO 50/50 blend recorded by the inversion−recovery pulse sequence.

For the 50/50 blends, although a single T_1^H value was observed for PEO in the blends, the value is very different from those observed for P(3HB-*co*-3HP) components except for the P(3HP)/PEO 50/50 blend. These differences in the T_1^H value between PEO and P(3HB-*co*-3HP) components seem to imply that these two components in the 50/50 blends were not intimately mixed, exhibiting immiscibility on this observation scale of NMR.

In fact, pure PEO, P(3HB), P(3HP), P(3HB-*co*-15%3HP), and P(3HB-*co*-25%3HP) are semicrystalline polymers. Furthermore, as has been reported,[34,35] the spectrum of PEO consists of narrow and broad components, corresponding to the amorphous and the crystalline phase, respectively. The amorphous phase of PEO has much longer ^{1}H T_2 and shorter ^{13}C T_1 values than the crystalline phase.[34] A curve-fitting program was used to obtain the integrated intensities and then they were used to calculate the T_1^H of two components in PEO. During the fitting the peak position and the peak shape of the crystalline and amorphous parts were fixed, but the widths and heights of the spectra were left as adjustable parameters. To compare the results of the curve fitting analysis to the ones obtained from thermal data of Table 2, the crystallinities of the PEO component in blends were calculated. For example, the crystallinities of the PEO component from the curve fitting data

Table 5. Proton Spin−Lattice Relaxation Times (T_1^H, s) for P(3HB)/PEO, P(3HB-*co*-15%3HP)/PEO, and P(3HB-*co*-25%3HP)/PEO Blends

sample	composition	CH_3(b1)	CH_2(b3)	CH(b2)	CO(b4)	CH_2(o1)
P(3HB)/PEO	P(3HB)	1.76(±0.01)	1.75(±0.02)	1.73(±0.02)	1.79(±0.01)	
	50/50	1.52(±0.01)	1.58(±0.01)	1.34(±0.04)	1.44(±0.02)	2.09(±0.07)[b]
	PEO					2.04(±0.02)[e]
P(3HB-*co*-15%3HP)/PEO	P(3HB-*co*-15%3HP)	1.64(±0.01)	1.60(±0.03)	1.59(±0.01)	1.61(±0.06)	
	50/50	1.41(±0.02)	1.48(±0.01)	1.47(±0.12)	1.53(±0.06)	2.00(±0.08)[c]
	PEO					2.04(±0.02)[e]
P(3HB-*co*-25%3HP)/PEO	P(3HB-*co*-25%3HP)	1.19(±0.03)	1.16(±0.02)	1.16(±0.06)	1.17(±0.06)	
	50/50	1.17(±0.02)	1.14(±0.02)	1.15(±0.08)	1.15(±0.03)	1.95(±0.10)[d]
	PEO					2.04(±0.02)[e]

[a] Some T_1^H values of crystalline and amorphous parts of PEO were calculated from the integrated intensities obtained by curve fitting method. The T_1^H values of crystalline and amorphous parts of PEO, respectively, are given in footnotes *b*−*e*. [b] 3.60(±0.28) and 1.32(±0.09) in P(3HB)/PEO 50/50 blend; [c] 3.46(±0.19) and 1.25(±0.04) in P(3HB-*co*-15%3HP)/PEO 50/50 blend; [d] 2.55(±0.31) and 1.18(±0.06) in P(3HB-*co*-25%3HP)/PEO 50/50 blend; [e] 3.40(±0.20) and 1.14(±0.04) in PEO homopolymer.

Table 6. Proton Spin−Lattice Relaxation Times (T_1^H, s) for P(3HP)/PEO Blend[a]

sample	composition	CH_2(p1)	CH_2(p2)	CO(p3)	CH_2(o1)
P(3HP)/PEO	P(3HP)	3.02(±0.01)	3.01(±0.02)	3.06(±0.06)	
	50/50	2.01(±0.08)	2.10(±0.02)	1.88(±0.04)	2.20(±0.09)[b]
	PEO				2.04(±0.02)[c]

[a] See the footnotes for Table 5. [b] T_1^H value of amorphous parts of PEO in P(3HP)/PEO 50/50 blend are 2.31(±0.16). [c] T_1^H values of crystalline and amorphous parts of PEO homopolymer are 3.40(±0.20) and 1.14(±0.04), respectively.

and DSC thermal data, respectively, were 82% and 79% in P(3HB)/PEO 50/50 blend; 66% and 71% in P(3HB-*co*-15%3HP)/PEO 50/50 blend; 82% and 70% in P(3HB-*co*-25%3HP)/PEO 50/50 blend; and 75% and 73% in PEO homopolymer. It is indicated that the two methods are in good agreement. (The difference between two data points in the P(3HB-*co*-25%3HP)/PEO 50/50 blend is attributed to comparatively poor *S*/*N* ratio and an effect of 3HP signal of noise level.)

The T_1^H value of pure semicrystalline PEO is 2.04(±0.02), but by such curve-fitting analysis, those values of crystalline and amorphous parts of the PEO homopolymer were estimated to be 3.40(±0.20) and 1.14(±0.04), respectively. It is noteworthy that T_1^H values of the respective carbon sites of P(3HB-*co*-3HP) components for all 50/50 blend systems decrease despite the longer T_1^H value(2.04) of PEO (from 1.73−1.79 to 1.34−1.58 for P(3HB)/PEO blend; from 1.59−1.64 to 1.41−1.53 for P(3HB-*co*-15%3HP)/PEO blend; and from 1.16−1.19 to 1.14−1.17 for P(3HB-*co*-25%3HP)/PEO blend). Thus, it should be reasonable to attribute the anomaly to averaging relaxation rate $(T_1^H)^{-1}$ of a homogeneous blend of P(3HB-*co*-3HP) and PEO in amorphous phase in that the T_1^Hs of all P(3HB-*co*-3HP) (co)polymers decrease in ranges between 1.14, T_1^H of amorphous part of PEO, and those of homo(co)polymers. For P(3HP)/PEO 50/50, it is also natural to show decrease of T_1^H values of each carbon site for P(3HP) component and increase of that of PEO part for P(3HP)/PEO 50/50 blend in which P(3HP) have relatively large T_1^H. The results suggest that the binary blends (at least in case of 50/50) are not phase-separated completely but are miscible to some extent, and the crystalline phase for each component of blends exists in the samples.

In addition to the discussion concerning the phase behavior of the blends discussed above, useful quantitative information about the domain size can be obtained from the equation[36]

$$\langle r^2 \rangle = 6D_s T \tag{4}$$

where $\langle r^2 \rangle$ is the mean square diffusive path-length and D_s is the spin diffusion constant which in the common case of a polymer is of the order of 10^{-16} m^2 s^{-1}. T is the time for a fundamental step in the random walk and has the value of T_1^H in this case. On the basis of eq 5 and the T_1^H values of 50/50 blends, it can be estimated that the two components of 50/50 blends were mixed over a range greater than 30−40 nm in the 50/50 blends of PEO with P(3HB), P(3HB-*co*-15%3HP), P(3HB-*co*-25%3HP), and P(3HP).

Conclusion

The T_m of the P(3HB), P(3HP), and P(3HB-*co*-3HP) copolymers in the binary blends with PEO decreased with the increase of the PEO content. Those of PEO also decreased with the increase of the partner component. Only one glass transition was observed in the DSC trace of each blend, in agreement with the Wood equation. The DSC thermal behavior of the blends indicated that PEO was miscible with P(3HB), P(3HP), and P(3HB-*co*-3HP) copolymers—irrelative to the 3HP content—in the amorphous phase over the whole composition range. Additionally, it should be reasonable to note that the crystallization of blend component followed by phase separation exerted much influence on the phase structure of blends. It is also found that the crystalline structure depend on the molecular mobility and the crystallization rate which are changed with 3HP content and blending compositional ratio.

For the proton spin−lattice relaxation behavior, it revealed that the 50/50 binary blends were phase-separated, due to the presence of a crystalline phase, but miscible to some extent. Two components in these blends were found to be mixed over a range greater than 30−40 nm, with two crystalline phases and an amorphous phase of the two miscible components coexisting.

Acknowledgment. This work was partially supported by a Grant-in-Aid for Scientific Research on Priority Area, "Sustainable Biodegradable Plastics", No.11217205 (2001) from the Ministry of Education, Science, Sports, and Culture (Japan).

References and Notes

(1) Doi, Y. *Microbial Polyester;* VCH Publisher: New York, 1990.
(2) Holmes, P. A. In *Developments in Crystalline Polymers*; Bassett, D. C., Ed.; Elsevier: London, 1988; Vol. 2.
(3) Anderson, A. J.; Dawes, E. A. *Microbiol. Rev.* **1990**, *54*, 450.
(4) Inoue, Y.; Yoshie, N. *Prog. Polym. Sci.* **1992**, *17*, 571.
(5) Howells, E. M. *Chem. Ind.* **1982**, 508.
(6) King, P. P. *Chem. Technol. Biotechnol.* **1982**, *32*, 2.
(7) Holmes, P. A. *Phys. Technol.* **1985**, *16*, 32.
(8) Avella, M.; Martuscelli, E. *Polymer* **1988**, *29*, 1731.
(9) Avella, M.; Martuscelli, E.; Greco. P. *Polymer* **1991**, *32*, 1647.
(10) Avella, M.; Martuscelli, E.; Ramio. M. *Polymer* **1993**, *34*, 3234.
(11) Choi, H. J.; Park, S. H.; Yoon, J. S.; Lee, H.-S.; Choi, S. J. *Polym. Eng. Sci.* **1995**, *35*, 1636.
(12) Park, S. H.; Lim, S. T.; Shin, T. K.; Jhon, M. S. *Polymer* **2001**, *42*, 5737.
(13) Kumagai, Y.; Doi, Y. *Polym. Degrad. Stab.* **1992**, *36*, 241.
(14) He, Y.; Asakawa, N.; Inoue, Y. *Polym. Int.* **2000**, *49*, 609.
(15) Cao, A.; Kasuya, K.; Abe, H.; Doi, Y.; Inoue, Y. *Polymer* **1998**, *39*, 4801.
(16) Na, Y. H.; Arai, Y.; Asakawa N.; Yoshie N.; Inoue, Y. *Macromolecules* **2001**, *34*, 4834.
(17) Wang, Y.; Ichikawa, M.; Cao. A.; Yoshie, N.; Inoue. Y. *Macromol. Chem. Phys.* **1999**, *200*, 1047.
(18) Arai, Y.; Cao, A.; Yoshie. N.; Inoue. Y. *Polym. Int.* **1999**, *48*, 1219.
(19) Gordon, M.; Taylor, J. S. *J. Appl. Chem.* **1952**, *2*, 493.
(20) Wood, L. A. *J. Polym. Sci.* **1958**, *28*, 319.
(21) He, Y.; Asakawa, N.; Inoue, Y. *J. Polym. Sci., Polym. Phys. Ed.* **2000**, *38*, 1848.
(22) Runt, J. P. *Macromolecules* **1981**, *14*, 420.
(23) Alfonso, G. C.; Russell, T. P. *Macromolecules* **1986**, *19*, 1143.
(24) Martuscelli, E.; Silvestre, C.; Addaonizio, M. L.; Amelino, L. *Makromol. Chem.* **1986**, *187*, 1557.
(25) Barham, P.; Keller, A. J.; Otun, E. L.; Holmes, P. A. *J. Mater. Sci.* **1984**, *28*, 2781.
(26) Talibuddin, S.; Wu, L.; Runt, J.; Lin, J. S. *Macromolecules* **1996**, *29*, 7527.
(27) Wu, L.; Lisowski, M.; Talibuddin, S.; Runt, J. *Macromolecules* **1999**, *32*, 1576.
(28) Fleiming, W. W.; Lyerla, J. R.; Yannoni, C. S. In *NMR and Macromolecules, Sequence, Dynamics, and Domain Structure*; Randall, J. C.; Ed.; ACS Symposuim Series 247; American Chemical Society: Washington, DC, 1984.
(29) Rothwell, W. P.; Waugh, J. S. *J. Chem. Phys.* **1981**, *74*, 2721.
(30) McBrierty, V. J.; Douglass, D. C. *J. Polym. Sci., Macromol. Rev.* **1981**, *16*, 295.
(31) Linder, M.; Hendrichs, P. M.; Hewitt, J. M.; Massa P. J. *J. Chem. Phys.* **1985**, *82*, 1585.
(32) Parmer, J. F.; Dickenson, L. C.; Chien, J. C. W.; Porter, R. S. *Macromolecules* **1989**, *22*, 1078.
(33) McBrierty, V. J.; Packer, K. J. *Nuclear Magnetic Resonance in Solid Polymer*; Cambridge University Press: Cambridge, U.K., **1993**.
(34) Zhang, X.; Takegoshi, K.; Hikichi, K. *Macromolecules* **1992**, *25*, 2336.
(35) Schantz, S. *Macromolecules* **1997**, *30*, 1419.
(36) Kwak, S.; Kim, J.; Kim, U. *Macromolecules* **1996**, *29*, 3560.

MA011530Y